

## Ferroelectricity of a bent-core material with cholesteryl terminal chain

G. Liao,<sup>1</sup> I. Shashikala,<sup>2</sup> C. V. Yelamagad,<sup>2</sup> D. S. Shankar Rao,<sup>2</sup> S. Krishna Prasad,<sup>2</sup> and A. J. Jáklí<sup>1</sup>

<sup>1</sup>*Chemical Physics Interdisciplinary Program and Liquid Crystal Institute, Kent State University, Kent, Ohio 44242, USA*

<sup>2</sup>*Centre for Liquid Crystal Research, Jalahalli, Bangalore 560 013, India*

(Received 10 February 2006; published 1 May 2006)

We have studied the phase sequence and physical properties of an asymmetric bent-core material with a chiral rigid cholesteryl moiety, and a flexible achiral alkyl side chain at the other end. The combination of the achiral bent core with the chiral cholesteryl unit results in properties different from those of both the usual calamitic and bent-core materials. We find that the presence of the bent core unit induces a wide-temperature-range optically isotropic (probably BPIII) mesophase between the isotropic and cholesteric (chiral nematic) phases. Below the cholesteric phase a ferroelectric smectic- $C^*$  structure occurs in which the bent-core units do not seem to form a polar close packing.

DOI: [10.1103/PhysRevE.73.051701](https://doi.org/10.1103/PhysRevE.73.051701)

PACS number(s): 61.30.Eb, 61.30.Cz, 61.30.Gd, 64.70.Md

### INTRODUCTION

Liquid crystals of rod-shaped molecules show manifestation of mesoscopic chirality when they contain chiral molecules, such as cholesteryl derivatives. These materials usually form a chiral nematic ( $N^*$ ) phase, which possess helical structures with the pitch ranging from submicrometers to hundreds of micrometers, representing the transfer of chirality from molecular to mesoscopic scales. In addition to the chiral nematic phase, chiral liquid crystals may also form smectic and twisted grain boundary phases. Smectic phases exhibit helical structures only if the director is tilted with respect to the smectic layers (e.g., the chiral smectic  $C^*$  or  $SmC^*$  phase). In this case the simultaneous molecular chirality and director tilt lead to the appearance of macroscopic polarization [1], which can be switched with electric fields, thus showing ferroelectricity. The research during the last decade revealed that tilted smectic phases of bent-core molecules [2] possess mesoscopic layer chirality [3] even when the molecules do not contain chiral centers. This is the result of the polar packing of the bent cores and the simultaneous tilt of the molecular plane with respect to the layer normal. Chirality can also be introduced when one or more chiral carbons are incorporated in such molecules, for example in the hydrocarbon terminal chains [4–6], within the bent core [7–9] or by addition of chiral dopants [3,10]. Recently it was shown that when one or more chiral carbons are incorporated in the molecules, either in the hydrocarbon terminal chains, or by addition of chiral dopants, two kinds of polarization  $P_b$  (due to the close packing of the bent-shape molecules) and  $P_c$  (due to the chiral and tilted molecular structure), can coexist [11].

In this paper we describe studies on a chiral bent-core substance, which is terminated by an achiral alkyl side chain at one end and by a chiral cholesteryl moiety at the other end. This molecule combines the achiral bent-core unit with a chiral end chain, and also introduces asymmetry, since one end is rigid and bulky, whereas the other one is flexible and much thinner. In a smectic phase the first property may result in an interplay between the polarization  $P_c$  due to the chiral unit and the polarization  $P_b$  due to the polar packing of the

bent cores, such as that reported by Binet *et al.* [11]. In addition the molecular asymmetry might result in nanoseparation of the structure, i.e., the cholesterol groups of different molecules within one layer would be positioned in the same direction, leading to a longitudinal polarization  $P_l$  along the layer normal [12]. Due to the pear shape of these molecules, however, such an order would be spontaneously splayed and may destroy the polar packing leaving only  $P_c$  to be nonzero. In the investigations reported here it is observed that the latter scenario is realized and the material has only the polarization due to the tilt and chirality introduced by the cholesteryl units.

### EXPERIMENTS

The chemical structure of the studied material 4-(3-(4-(2-hydroxy-4-(5-cholesteryloxy)carbonyl) pentyloxy)benzylideneamino benzoyloxy)phenoxy)carbonyl)phenyl 4-(decyloxy)benzoate is shown in Fig. 1. The synthesis of this and similar substances with their phase sequences will be published separately [13].

To express the simultaneous presence of the bent core (B) and the chiral cholesterol unit (Ch) we shall call this material BCh.

To test the phase sequence of the material differential scanning calorimetry (DSC) experiments have been carried out with a Perkin-Elmer DSC-7. The dielectric properties were tested in the frequency range 100 Hz–1 MHz by a precision impedance analyzer (Quadtech 1920). The temperature dependences of the optical transmittance of samples sandwiched between two indium tin oxide-coated (ITO) glass plates separated by 5- $\mu\text{m}$ -thick spacers were monitored simultaneously under a polarizing microscope (Olympus BX60) while measuring the dc resistance using a digital multimeter. The x-ray diffraction experiments were done using  $\text{Cu } K\alpha$  radiation ( $\lambda=1.5418 \text{ \AA}$ ) from a fine focus sealed-tube generator in conjunction with double-mirror focusing optics. The mirror optics provides a nearly parallel beam over a long working distance. The diffracted x ray was detected by an image plate detector (MAC Science, Japan, model DIP 1030) with an effective resolution of  $100 \times 100 \mu\text{m}^2$ .

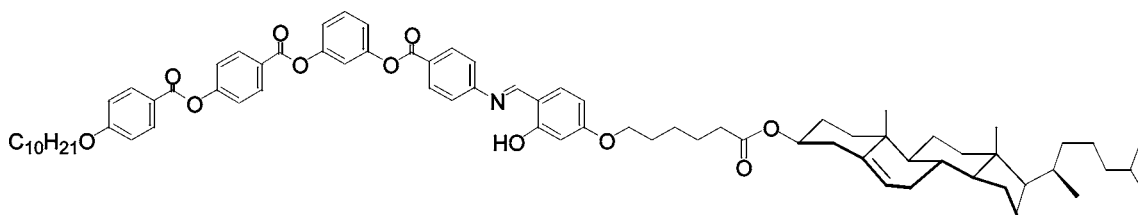


FIG. 1. The molecular structure and the phase sequence of the material BCh.

## RESULTS

DSC measurements indicate only one mesophase ( $M_1$ ) in heating and two mesophases ( $M_1$  and  $M_2$ ) in cooling at 5 °C/min rates. The transition temperatures and enthalpies (in parentheses) in cooling are  $I$  174.5 °C (0.8 J/g)  $M_1$  138.3 °C (10.5 J/g)  $M_2$  52 °C glass. In heating from the crystalline phase it directly melts to the  $M_1$  phase at 151.1 °C (33.4 J/g), which then becomes an isotropic liquid at 175.5 °C (0.8 J/g). This shows that the  $M_2$  phase is monotropic.

In the temperature range corresponding to the  $M_1$  phase from the DSC measurements the x-ray data show diffuse peaks at both small and wide angles indicating a three-dimensional fluid state (Fig. 2). The sharp (resolution-limited) low-angle peak in conjunction with a diffuse peak in the wide-angle region in the  $M_2$  phase indicates that the phase is a smectic. Considering the all-*trans* configuration length of the molecule (6.6 nm) and 120° opening angle at the center, the calculated layer spacing of 4.93 nm suggests a tilt angle of 42°, which is not uncommon in the case of materials exhibiting direct nematic to smectic-*C* transitions. We will see later that this assumption is consistent with the electro-optical investigations, as well.

The temperature dependence of the integrated optical intensity between crossed polarizers indicates an additional phase transition at 152 °C in cooling (and at 166 °C during heating) that was not observable by DSC and x-ray measurements. Tentatively we will label the phase in the higher-temperature range of the earlier assigned  $M_1$  as  $M_{1a}$  and the

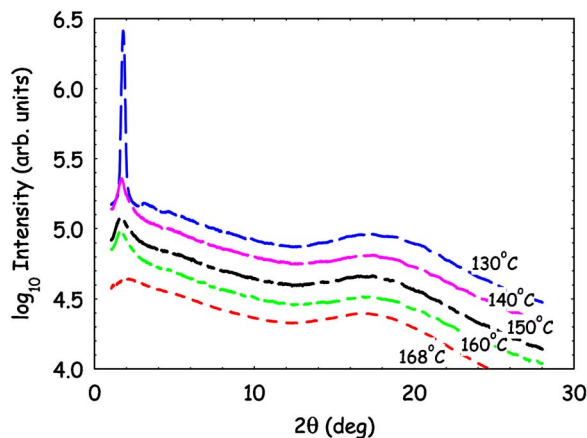


FIG. 2. (Color online) X-ray diffraction patterns at different temperatures measured at equilibrium temperatures starting at the highest temperature (isotropic phase).

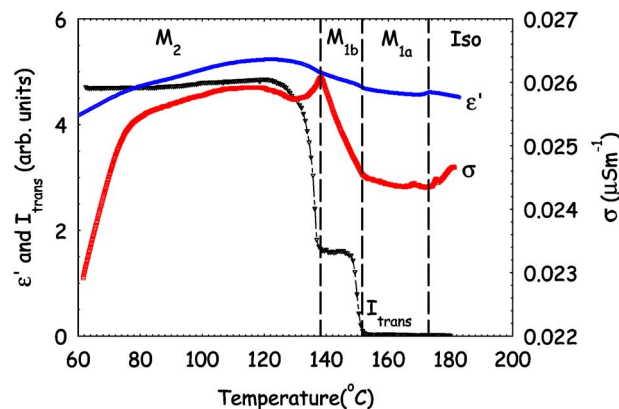
one at the lower-temperature range as  $M_{1b}$ . In thin ( $d < 10 \mu\text{m}$ ) cells with planar anchoring the birefringence increases abruptly from zero in the  $M_{1a}$  to a value in the  $M_{1b}$ , that is about one-third of the transmittance observed in the tilted smectic  $M_2$  phase. The electric conductivity of the same cell measured at 100 kHz increases monotonically starting at 152 °C and reaching a maximum upon the transition to the smectic phase (see Fig. 3).

The dielectric constants were measured with cells having planar as well as homeotropic anchoring in the frequency range between 100 Hz and 1 MHz, and no relaxation was observed. Interestingly, the absolute values of the dielectric constants are relatively small in all the phases under both alignment conditions. The values obtained in the two geometries are nearly identical indicating that the director structures in the bulk are independent of the surface alignment. In spite of the relatively small temperature variation the iso- $M_{1a}$ - $M_{1b}$ - $M_2$  phase transitions are clearly seen and the transition temperatures match well with the optical and conductivity measurements (see Fig. 3).

Polarizing microscopic textures of the planar cells at selected temperatures are shown in Fig. 4. The dark blue fog-type texture observed in the  $M_{1a}$  phase resembles the amorphous blue phase (BPIII). The texture in the  $M_{1b}$  phase is the oily streak texture typical of the cholesteric phase.

In cells with homeotropic anchoring both  $M_{1a}$  and  $M_{1b}$  phases appear to be dark between crossed polarizers.

To measure the pitch in the  $M_{1b}$  ( $N^*$ ) phase we have prepared Cano-wedge cells (wedge angle is  $2 \times 10^{-3}$ ). The pitch of the helix was determined by the periodicity of the Cano

FIG. 3. (Color online) Temperature dependences of the optical transmission  $I_{\text{trans}}$  (integrated area  $\sim 1 \text{ mm}^2$ ) measured in cooling at 1 °C/min rates; the electric conductivity  $\sigma$  and dielectric constant  $\epsilon'$  measured at 100 kHz of a 5- $\mu\text{m}$ -thick sample with planar boundary conditions.

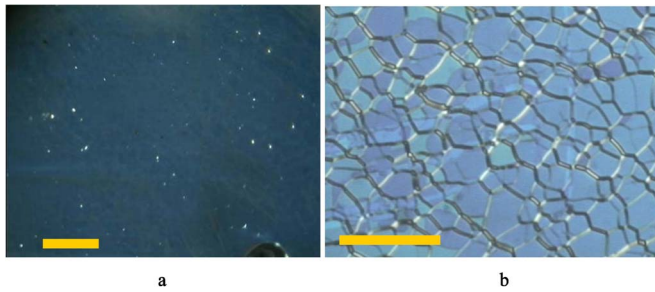


FIG. 4. (Color online) Textures in the  $M_{1a}$  and  $M_{1b}$  phases of a 5- $\mu\text{m}$ -thick film. (a) Blue fog-type texture at 168  $^{\circ}\text{C}$ . (b) Oily streak texture at  $T=145$   $^{\circ}\text{C}$ . Bars are 100  $\mu\text{m}$  long.

lines to be about 0.3  $\mu\text{m}$ . No Cano lines can be observed in the  $M_{1a}$  range. The pitch values determined in this way are consistent with those deduced from the reflection spectra (not shown) which have maxima in the visible 450–500 nm wavelength range.

Typical textures in the  $M_2$  phase in planar anchoring conditions are shown in Fig. 5. They do not resemble that of smectics with planar anchoring, where either fan-shape or focal-conic domains are usually observed. In our case they look rather like the schlieren textures decorated by a chiral pattern indicating that the smectic layers are not perpendicular to the substrates [see Fig. 5(a)]. The textures in homeotropically treated cells look very similar to those with planar anchoring [see Fig. 5(b)].

On applying low-frequency electric fields we have observed a rotation of the optical axis practically without any threshold in the form of rotation of the Maltese crosses with the frequency of the electric field with angles that are proportional to the voltage applied. After removal of  $E < 10$   $\text{V}/\mu\text{m}$  fields the original textures shown in Figs. 5(a) and 5(b) recovered completely reversibly. However after

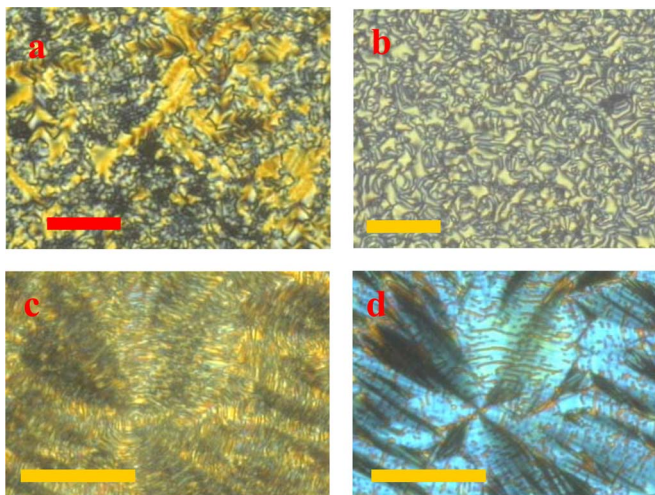


FIG. 5. (Color online) Typical textures of 5  $\mu\text{m}$  films. Upper row: Virgin textures at 130  $^{\circ}\text{C}$  with planar (a) and homeotropic (b) alignment coating. Bottom row: Textures with planar anchoring at 105  $^{\circ}\text{C}$  after realignment by  $E=15$   $\text{V}/\mu\text{m}$ ,  $f=23$  Hz electric fields; at zero electric field (c) and under applied  $E=+20$   $\text{V}/\mu\text{m}$  (d). Bars are 0.1 mm long.

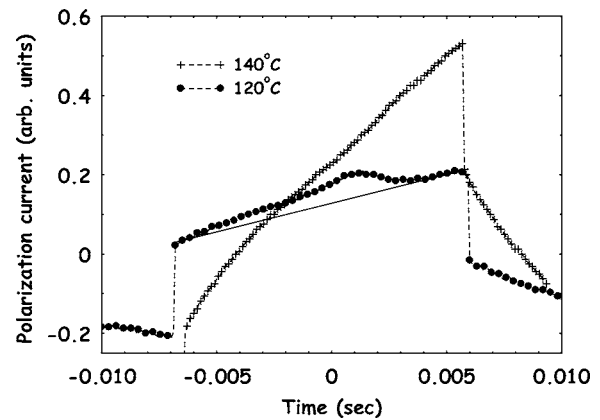


FIG. 6. Time dependence of the electric current flowing through the sample under triangular electric voltage excitation of  $E = 10$   $\text{V}/\mu\text{m}$  fields in the  $M_2$  phase at 120  $^{\circ}\text{C}$  and in the cholesteric phase at 140  $^{\circ}\text{C}$ .

switching the material with low-frequency fields of amplitude  $E > 12$   $\text{V}/\mu\text{m}$ , focal-conic type defects appeared gradually, and then remained stable even after field removal. For the thicker cells ( $d > 5$   $\mu\text{m}$ ) fine stripes, separated by about 1–3  $\mu\text{m}$  distances, appear first [see Fig. 5(c)] that eventually fill the whole area and the stripes cannot be resolved, indicating that the fully formed helical structure has a submicrometer-size pitch. The pitch decreases at lower temperatures and the helix cannot be resolved by the microscope below about 80  $^{\circ}\text{C}$ . When an electric field is applied the helix becomes unwound above a temperature-dependent threshold (2  $\text{V}/\mu\text{m}$  at 136  $^{\circ}\text{C}$  and 20  $\text{V}/\mu\text{m}$  at 100  $^{\circ}\text{C}$ ). Above these fields the switching angle is about 90 $^{\circ}$ , indicating tilt angle of about 45 $^{\circ}$  [see Fig. 5(d)] in good agreement with the x-ray results. In this state the rotation of the optical axis can be seen only by inserting a wave plate between the sample and analyzer.

The time dependence of the electric current under a triangular wave voltage is shown in Fig. 6 in both the smectic and cholesteric phases. The observed current peak in the smectic phase indicating the presence of ferroelectricity disappears upon heating to the cholesteric phase, ruling out any ionic origin for its appearance. The magnitude of the area of the current peak above a background that is linear in time, corresponding to the Ohmic current, gives  $P_0 \sim 30$   $\text{nC}/\text{cm}^2$ , which is much smaller than that typical for bent-core smectics.

To test the influence of strong electric fields on the dielectric anisotropy of the material, we have measured the dielectric constant before and after applying a 23 Hz square wave field of magnitude 16  $\text{V}/\mu\text{m}$ , for 10 min at 122  $^{\circ}\text{C}$ . The measurement was done in the heating mode in which the transition from the  $M_{1b}$  to  $M_{1a}$  phase occurred only at 166  $^{\circ}\text{C}$  (see Fig. 7). It can be seen that in the  $M_2$  phase the dielectric constant is smaller in the virgin cell than in the field-treated state. There is basically no difference in the  $M_{1a}$  phase, indicating again that it is a macroscopically isotropic structure.

## DISCUSSION

Textural observations on flat and wedge-shape cells clearly show that the  $M_{1b}$  phase is a cholesteric phase with a



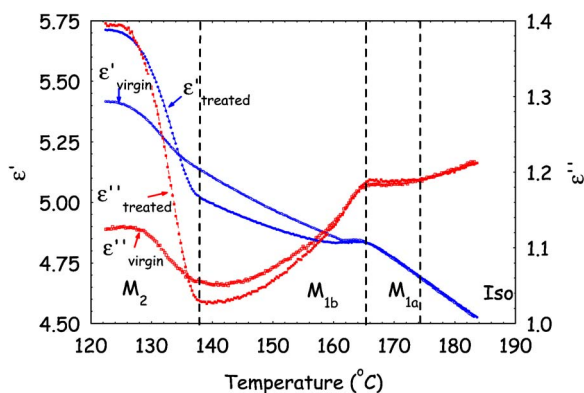


FIG. 7. (Color online) Temperature dependences measured in heating starting in the  $M_2$  phase at 122 °C of the real ( $\epsilon'$ ) and imaginary ( $\epsilon''$ ) dielectric constants measured in 2  $\mu\text{m}$  cells with substrates preferring homeotropic anchoring for rod-shaped molecules. In the virgin cell no electric field was applied previously. In the treated cell the data were taken after a 16 V/ $\mu\text{m}$ , 23 Hz square wave field was applied for 10 min at 122 °C.

short pitch in the range of 0.3  $\mu\text{m}$ . The observation that the  $M_{1a}$  phase is optically isotropic and has a foggy texture indicates an amorphous BPIII structure (double-twist cylinders with arbitrary orientation) [14]. Interestingly the thermal range is much wider than that observed usually for BPIII phases. We note that in some respects this situation is similar to the blue phase induced by doping chiral nematic liquid crystals with nonchiral bent-core molecules [15], where the bent-core molecules assumed an asymmetric configuration thereby acting as chiral dopants. In our case, instead of the bent-core dopant we have bent-core units chemically attached to the chiral cholesterol unit. We note that a similarly wide temperature range (although only monotropic) BPIII phase was observed recently on T-shaped molecules [16]. The structures and stabilities of the BPIII phase in this material and in other homologues will be reported and discussed in detail elsewhere [13].

In this paper we focus on the nature of the  $M_2$  phase. The x-ray results indicate that this phase has a tilted fluid smectic structure, of either banana-shaped chiral tilted polar ( $\text{SmCP}^*$ ) or calamitic  $\text{SmC}^*$  type. In case of close-packed bent-core structures the layer polarization is typically well over 100 nC/cm<sup>2</sup>, and the switching usually requires thresholds of about 3 V/ $\mu\text{m}$  or larger. The low value of the ferroelectric polarization and the low threshold for switching therefore indicate that the spontaneous polarization is solely due to the chirality and tilt, and not the polar packing of the bent-cores, i.e., the  $M_2$  phase is identical with a chiral smectic- $C^*$  phase. This probably is due to the bulky cholesterol units which have to alternate to avoid splay of the director or bend of the layers, thereby preserving the head-tail symmetry.

The 45° tilt angle observed by the electro-optical and x-ray studies is usual for  $\text{SmC}^*$  materials with a direct  $N^*$ - $\text{SmC}^*$  transition.

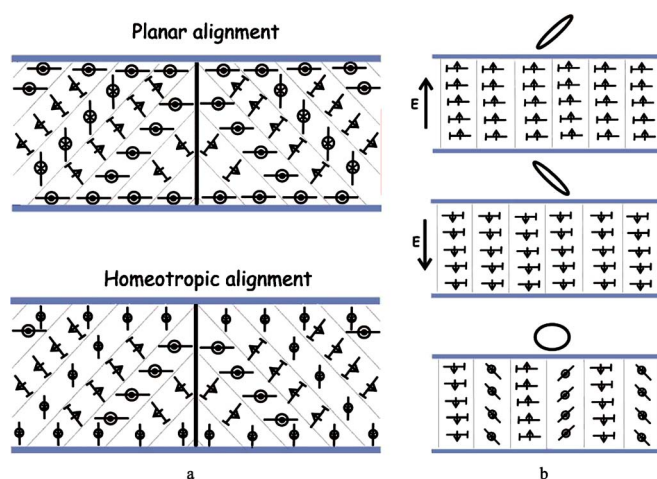


FIG. 8. (Color online) Proposed layer and director structures of the virgin and realigned samples. The heads of the nails represent tilting of the molecules toward the plane of the drawing. The symbols ( $\uparrow$ ,  $\downarrow$ ,  $\otimes$ ,  $\odot$ ) indicate the electric polarization pointing (up, down, inside, and outside), respectively. (a) Virgin cells with planar and homeotropic surface anchoring conditions. (b) Layer and director structures in the realigned bookshelf geometries under electric fields in different polarities (upper two cells) and at zero electric field (bottom cell). The ellipses above the cells illustrate the projection of the optical indicatrix on the substrates. In the two unwound states the optical axes make  $\pm 45^\circ$  with respect to the polarizers and in the fully formed helical structures the texture is almost quasi-isotropic.

Due to the small pitch and the 45° tilt angle of the molecules in both surface alignments the bulk alignments are basically the same, explaining the similarities between the measured dielectric constants on both types of cells (see Fig. 8). In this case, because of the helix, the director periodically varies between vertical and horizontal positions.

The observation that at high fields the focal conic textures appeared and the measured dielectric constant increased as compared to that of the virgin samples points to a permanent realignment of the layers to the bookshelf structure. The ferroelectric polarization peak appears only in this state and the switching angle is  $2 \times 45^\circ$  after helix unwinding. The textures in this bookshelf geometry together with the projection of the effective optical indicatrix on the substrates are illustrated in Fig. 8(b).

In summary, we have studied the effect of the combination of the achiral bent-core unit with the chiral cholesterol unit on the phase sequence and physical properties of the material. We find that the presence of the bent core induces a wide temperature range optically isotropic (probably BPIII blue phase) structure between the isotropic fluid and cholesteric phases. We have also found a ferroelectric  $\text{SmC}^*$  phase, in which the bent-core unit does not seem to form a polar close packing.

- [1] R. B. Meyer, L. Liebert, L. Strzelecki, and P. Keller, *J. Phys. (France)* **36**, L69 (1975).
- [2] T. Niori, T. Sekine, J. Watanabe, T. Furukawa, and H. Takezoe, *J. Mater. Chem.* **6**, 1231 (1996).
- [3] D. R. Link, G. Natale, R. Shao, J. E. MacLennan, N. A. Clark, E. Körblova, and D. M. Walba, *Science* **278**, 1924 (1997).
- [4] M. Nakata, D. R. Link, F. Araoka, J. Thisayukta, Y. Takanishi, K. Ishikawa, J. Watanabe, and H. Takezoe, *Liq. Cryst.* **28**, 1301 (2001).
- [5] K. Kumazawa, M. Nakata, F. Araoka, Y. Takanishi, K. Ishikawa, J. Watanabe, and H. Takezoe, *J. Mater. Chem.* **14**, 157 (2004).
- [6] C.-K. Lee, S.-S. Kwon, T.-S. Kim, E.-J. Choi, S.-T. Shin, W.-C. Zin, D.-C. Kim, J.-H. Kim, and L.-C. Chien, *Liq. Cryst.* **30** 1401, (2003).
- [7] G. Gesekus, I. Dierking, S. Gerber, M. Wulf, and V. Vill, *Liq. Cryst.* **31**, 145 (2003).
- [8] J. P. F. Lagerwall, F. Giesselmann, M. D. Wand, and D. M. Walba, *Chem. Mater.* **16**, 3606 (2004).
- [9] R. Amarnath Reddy, B. K. Sadashiva, and U. Baumeister, *J. Mater. Chem.* **15**, 3303 (2005).
- [10] A. Jákli, S. Rauch, C. Binet, H. Sawade, and G. Heppke (unpublished).
- [11] C. Binet, S. Rauch, Ch. Selbmann, Ph. Bault, G. Heppke, H. Sawade, and A. Jákli, in *Proceedings of German Liquid Crystal Workshop, Mainz, 2003* (unpublished).
- [12] R. G. Petschek and K. M. Wiefeling, *Phys. Rev. Lett.* **59**, 343 (1987).
- [13] C. V. Yelamaggad, I. S. Shashikala, G. Liao, D. S. Shankar Rao, S. K. Prasad, Q. Li, and A. Jákli (unpublished).
- [14] H.-S. Kitzerow and C. Bahr, *Chirality in Liquid Crystals* (Springer-Verlag, New York, 2001).
- [15] M. Nakata, Y. Takanishi, J. Watanabe, and H. Takezoe, *Phys. Rev. E* **68**, 041710 (2003).
- [16] A. Yoshizawa, M. Sato, and J. Rokunobe, *J. Mater. Chem.* **15**, 3285 (2005).